Journal of Nuclear Materials 390–391 (2009) 127–131

Contents lists available at ScienceDirect

Journal of Nuclear Materials

journal homepage: www.elsevier.com/locate/jnucmat

Steady-state and transient hydrocarbon production in graphite by low energy impact of atomic and molecular deuterium projectiles

H. Zhang, F.W. Meyer *

Physics Division, Oak Ridge National Laboratory, Oak Ridge, TN 37831-6372, USA

ARTICLE INFO

PACS:
34.35.+a
52.20.Hv
79.20.−m
79.20.Rf

ABSTRACT

We report measurements of steady-state yields of methyl, methane and heavier hydrocarbons for deuterium atomic and molecular ions incident on ATJ graphite, HOPG, and a-C:D thin films in the energy range 10–200 eV/D. The yields were determined using a QMS technique in conjunction with calibrated hydrocarbon leaks. We have also studied transient hydrocarbon production and hydrogen (deuterium) re-emission for 80 and 150 eV/D D^+, D_2^+, and D_3^+ projectiles incident on ATJ graphite surfaces pre-loaded to steady state by 20 eV/D beams of the corresponding species. Immediately after starting the higher-energy beams, transient hydrocarbon and D_2 re-emission yields significantly larger than steady-state values were observed, which exponentially decayed as a function of beam fluence. The initial yield values were related to the starting hydrocarbon and deuterium densities in the prepared sample, while the exponential decay constants provided information on the hydrocarbon kinetic release and hydrogen (deuterium) detrapping cross-sections.

1. Introduction

Carbon-based materials are important constituents of plasma-facing components of present and future fusion devices [1]. For this reason, the physical and chemical sputtering behavior of carbon materials has been extensively studied [2]. Characterization of the hydrocarbon species emitted as a result of chemical sputtering and erosion is central to understanding and modeling of fusion plasma impurity content and transport and of wall lifetimes. Redeposition of such hydrocarbon species has serious consequences on the tritium inventory accumulated in future burning-plasma machines. While models have been developed to explain general features of chemical sputtering by energetic hydrogen ions and their isotopes [3–7], many details of the processes underlying chemical sputtering are still incompletely understood. The conversion step from CH_3 radical to CH_4 molecule during room-temperature-target chemical sputtering of graphite by energetic hydrogen ions has not been conclusively identified [8], and, moreover, has not been successfully incorporated into current chemical sputtering MD simulations [9,10]. The hydrocarbon release mechanism during room-temperature chemical sputtering is still the subject of discussion, ranging from projectile-induced kinetic ejection [3,9], to purely diffusive release [6,7]. In addition, there are unresolved technical issues leading to differences between various measurement techniques [11] for determination of the total C chemical sputtering yield.

In this article, we present measurements for steady-state methyl, methane, and heavier hydrocarbon production by 10–200 eV/D D^+, D_2^+, and D_3^+ ion impact on a range of different graphite materials: ATJ graphite, HOPG with two different basal plane orientations, and a-C:D thin films. In addition, we describe measurements of transient emission of D_2, and of CD_4, C_2D_2, and C_2D_4 resulting from impact of 80 and 150 eV/D D^+, D_2^+, and D_3^+ on ATJ graphite surfaces that have been prepared by exposure to large-fluence 20 eV/D deuterium-ion beams. In contrast to beam exposure of a virgin graphite surface, where deuterium and hydrocarbon emission levels are initially close to zero, and approach steady-state levels only after accumulation of large fluences, the initial emission levels for the beam-prepared surfaces significantly exceed steady-state levels. From these high initial levels, the emission transients rapidly decrease by simple exponential decay with a time constant, depending on beam flux, in the range 5–30 s. Using a simple model, cross-sections for incident-projectile-induced release of deuterium and hydrocarbons are deduced. Ion-induced release and detrapping of deuterium in D-beam-prepared graphite surfaces have been extensively studied for H, He, C, and N beams at keV and MeV energies [12–14].

2. Experiment

The experimental apparatus used in this work has been described previously [15,16]. All measurements were performed in

* Corresponding author.
E-mail address: meyerfw@ornl.gov (F.W. Meyer).

0022-3115/$ - see front matter © 2009 Elsevier B.V. All rights reserved.
doi:10.1016/j.jnucmat.2009.01.142

a floating potential ultra-high vacuum chamber with base pressures in the 10^{-8} Pa range, into which decelerated ion beams from an ECR ion source can be directed, as previously described [17]. A sensitive quadrupole mass spectrometer (QMS) was installed in the scattering chamber to detect the emission of deuterium, methyl radicals, and CD_4, C_2D_2, C_2D_4, C_2D_6, C_3D_6, and C_3D_8 hydrocarbons. The beam was well defined spatially (FWHM ~4 mm below 60 eV/D) and in energy. As discussed elsewhere [18], the energy spread of the decelerated beams was less than 10% down to a final energy of 10 eV and typically below 20% at lower energies, as measured using an electrostatic spherical sector spectrometer. Fluxes in excess of 1×10^{15} D/(cm^2 s) were obtained for energies as low as 10 eV/D. The deuterium-ion beams impacted the sample at normal-incidence.

The QMS, which was interfaced to a Macintosh-based data acquisition system, was used to measure mass distributions in the 1–80 amu mass range at fixed intervals in time, or alternatively, to follow the intensity of selected mass peaks vs. beam-exposure time. The evolution of peak intensities was measured vs. accumulated beam fluence until steady-state conditions were reached. The incident ion intensity was determined from a direct current reading on the target sample. The procedure used to deduce the partial chemical sputtering yields has been described in detail in Ref. [19]. It involves selection of an analysis mass for identification of each species of interest, determining and correcting for the possible interferences due to cracking of heavier hydrocarbons, and placing the production yields on an absolute scale using calibrated leaks. The procedure is expressed by the equation $\boldsymbol{y} = \mathbf{R}(\mathbf{C}^{-1}\boldsymbol{s})$, where $\boldsymbol{y}$ is the apparent production yield array for the selected hydrocarbons, $\mathbf{C}$ is the cracking pattern matrix, and $\mathbf{R}$ is the diagonal calibration matrix giving the conversion from QMS normalized peak height to production rate in particles/s. The vector $\boldsymbol{s}$ is the array of measured peak heights (normalized to the incident ion flux, expressed in particles/s) at each analysis mass. To obtain true partial chemical sputtering yields, the apparent yields must be corrected for wall contributions.

The ATJ graphite (UCAR Carbon Co.) and highly oriented pyrolytic graphite (HOPG) targets could be electron-beam heated from the rear. For these targets, sample annealing at temperatures in excess of 1200 °C was performed, as determined using a calibrated infrared (IR) thermal monitor, in order to reinitialize the sample after each measurement condition. The a-C:D thin films were ~250 nm thick and had an initial D/C content of ~30% as provided by IPP-Garching, and, with exception of initial chamber bake-out to 100–150° C for a period of 5 days, were not heated between beam exposures.

3. Results

Fig. 1 shows the ratio of CD_3 to CD_4 emission as function of normal-incidence D_2^+ ion impact energy for three different graphite targets. After determination of the chemical sputtering yields for the heavier hydrocarbon species to be discussed in the following paragraphs, their contribution to the mass 18 signal (by cracking in the QMS ionizer) was subtracted using the cracking patterns determined *in situ* from the various hydrocarbon calibrated leaks. For absolute calibration of the mass 18 intensity, it was assumed that the QMS response was identical to that at mass 20, and that the cross-sections for simple electron impact ionization of CD_3 and CD_4 were comparable. Since initial 'beam-on' transients were not measured for this mass peak, the mass 18 intensity could not be corrected for wall contributions [19], which for the CD_4 chemical sputtering signal could result in corrections of up to 30%.

Fig. 2 shows the summed steady-state C-production yields from CD_3 radicals plus CD_4, C_2D_2, C_2D_4, C_2D_6, C_3D_6, and C_3D_8 hydrocarbons from a variety of graphite targets by exposure to D^+, and D_2^+ and D_3^+ ions to fluences in excess of 10^{18}/cm^2. The masses used for identification of the stable hydrocarbons listed above were, in the same order, 20, 24, 30, 36, 46, and 34, respectively. Since we did not have a calibrated leak of C_3D_6, we estimated the QMS response from that for C_3D_8 by assuming comparable simple electron impact ionization cross-sections for the two species and then allowing for the different cracking intensities at the respective analysis masses. For comparison, the CD_4 yields resulting from D_2^+ impact on ATJ graphite are shown in the figure as well, both with and without corrections for wall contributions. Since many of the peak intensities at the analysis masses for the heavier hydrocarbons were low, poor signal-to-noise ratios prevented reliable estimation of wall contri-

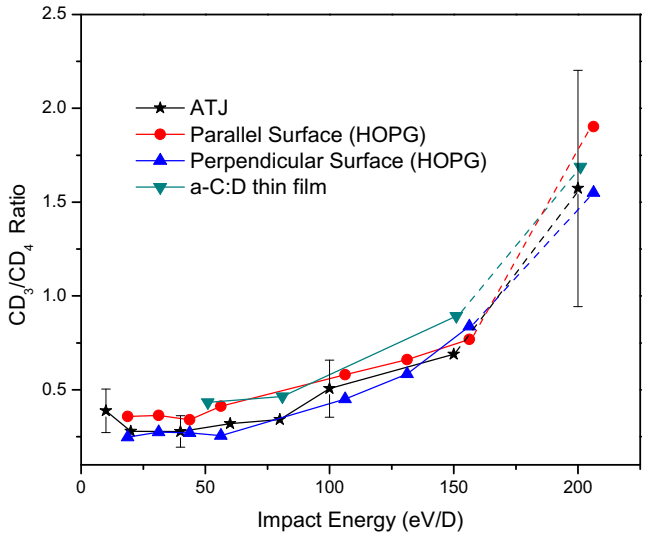

Fig. 1. Ratio of emitted CD_3 and CD_4 vs. ion impact energy for D_2^+ normally incident on four different room-temperature C targets.

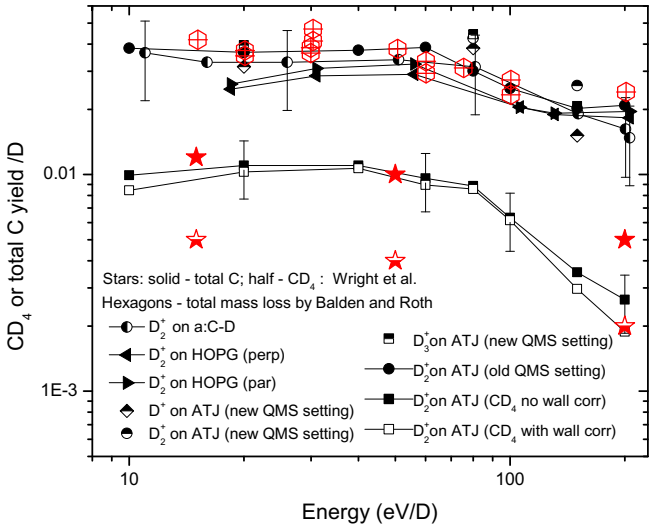

Fig. 2. Hydrocarbon yields summed over the species of the present study (CD_3, CD_4, C_2D_2, C_2D_4, C_2D_6, C_3D_6, and C_3D_8) for atomic and molecular deuterium ions incident on a number of different room-temperature graphite targets, uncorrected for wall contributions (see text); also shown are methane chemical sputtering yields for incident D_2^+ ions as function of energy, shown with and without correction for wall contributions. Also shown are the results of Wright et al. For methane and total C-production [22], and the total mass loss measurements of Balden and Roth [11]. (For interpretation of the references to colour in this figure legend, the reader is referred to the web version of this article.)

butions for these species. The total C-production yields are therefore shown without corrections for wall contributions.

In addition to the steady-state hydrocarbon yields, measurements were made of the initial transient D_2, CD_4, C_2D_2, and C_2D_4 signals observed immediately after the start of exposure of specially prepared ATJ graphite surfaces to 80 eV/D and 150 eV/D D^+, D_2^+, and D_3^+ beams. These measurements were made with new QMS multiplier settings, which increased signal levels at least a factor of 4. The ATJ graphite surface was prepared by 20 eV/D beams of the same species to steady state conditions, i.e. to accumulated fluences of a few times $10^{18}/cm^2$. This was followed, typically the next day, by exposure till steady-state conditions were reached of a higher-energy beam of the same species, during which the initial 'beam-on' transient signals were monitored. At the conclusion of each higher-energy beam-exposure, the sample was annealed to 1500 K to reinitialize the D inventory. Unlike the case of a virgin surfaces, where the selected mass signals started from initial levels significantly below steady-state values (the initial signal levels are determined by the particle reflection coefficient at the incident beam energy), for the surfaces prepared by low-energy beam exposure, initial levels were significantly above steady-state values, which then exponentially decayed. This behavior is illustrated in Fig. 3. Thermal desorption due to sample heating by the incident beam is expected to have no effect on the observed transients, since the ion-beam powers used did not exceed a few mW, and were at least four orders of magnitude lower than the e-beam powers used during active sample heating.

4. Analysis and discussion

4.1. Steady-state yields

The room-temperature relative CD_3 production yields shown in Fig. 1 are of interest for at least three reasons. First, it is a representative of radicals with very low sticking coefficients [21], which should be detectable even by QMS approaches that do not have direct line of sight detection geometries such as ours. Further, they can potentially contribute to the over-all C production, and thus must be included in comparisons with, e.g. total mass loss measurements [11]. Finally, they serve as a point of comparison to chemical sputtering calculations. While recent MD simulations [9,10] have shown very good agreement with experiment in the sum of CD_3 and CD_4 production, the radical contribution in the MD simulations dominated over CD_4 production by factors of at least 4. This may be further evidence for the missing step noted by Vietzke [8], in which during or after the ion-induced CD_3 release association of an additional D atom to the radical occurs, which may not be properly treated in the simulations. On the other hand, the present results indicate that the radical contribution is well below 50% of the combined CD_3 and CD_4 production. It is emphasized that the CD_3/CD_4 ratio shown in Fig. 1 is an upper limit, since it is not corrected for wall contributions. The present results are in good agreement with the [mass 18]/[mass 20] signal ratio found by Balden et al. [22] at 30 eV/D. It is noted that our values deduced at 200 eV/D have a greater uncertainty than the lower energy

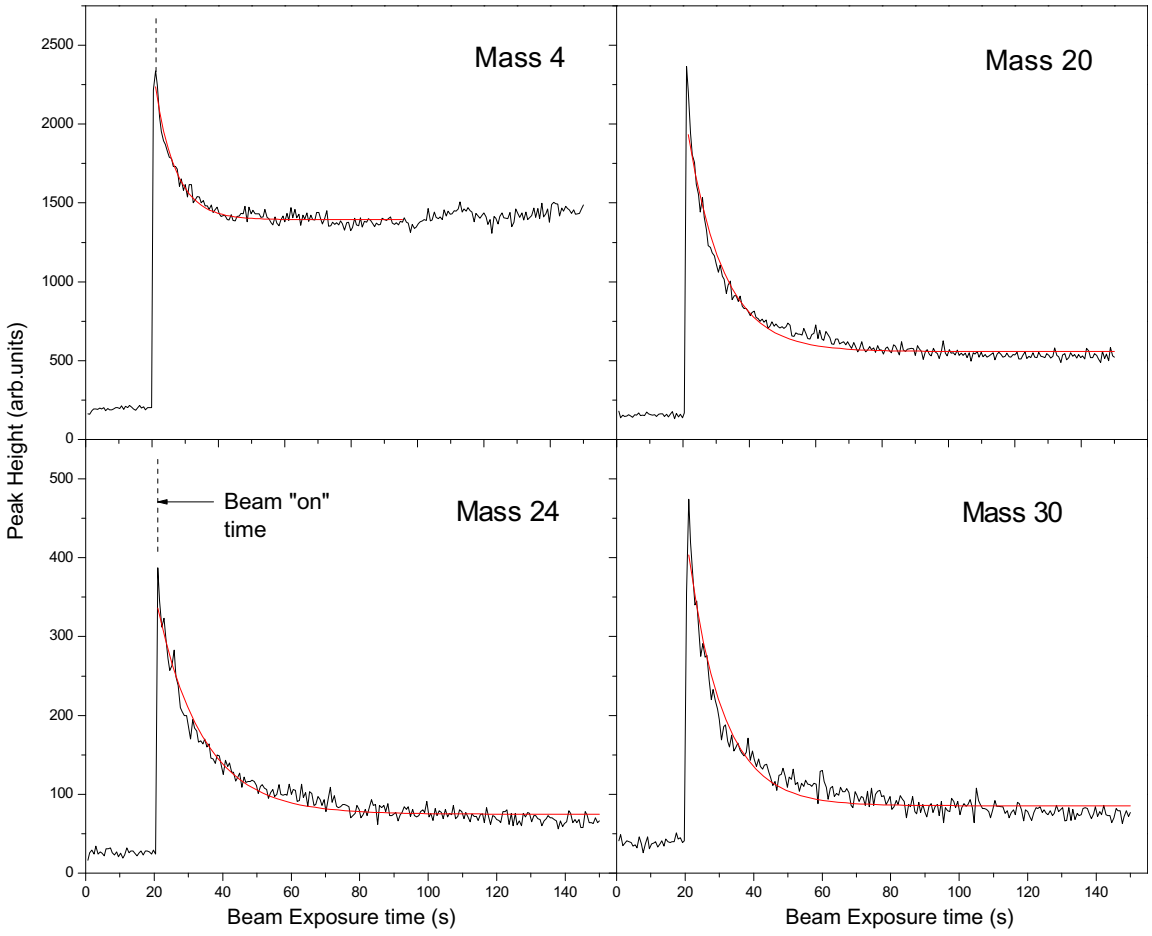

Fig. 3. Initial transients at mass 4 (D_2), 20 (CD_4), 24 (C_2D_2), and 30 (C_2D_4) for 150 eV/D D^+ ions incident on beam-prepared ATJ graphite, as function of beam-exposure time. The solid smooth lines are fits to the functional form $a + b\exp(-ct)$. The cross-sections deduced from the decay time constants are summarized in Table 1.

results because of strongly decreasing signal levels compared to background, a situation similar to that noted in [22].

As already mentioned the total C-production yields of Fig. 2 deduced from the hydrocarbons analyzed in the present study, including the CD_3 contribution just discussed, have not been corrected for wall contributions. In comparison to the similarly uncorrected CD_4 yields, also shown in the figure, it is seen, that at energies below ~100 eV/D, the total C-production yields are a factor of 3–4 higher. This factor is higher than that determined from the data of Mech et al. [20], which was closer to a factor of two. We are not able to assess if the difference is due to significantly higher wall contribution corrections required for the heavier hydrocarbon species in comparison to CD_4 or due to differences in calibration factors for the heavier species. It is noted that the methane yields quoted by Mech et al. [20] and ours agree quite well at 50 eV/D, but decrease rather steeply with decreasing energy, in contrast to ours, which are almost flat at energies below 70 eV/D. Later measurements by Wright et al. [23] showed a similarly flat energy dependence at low energies as ours, but are a factor of two lower at 50 eV/D than those of Mech et al. [20]. Fig. 2 also shows the mass loss measurements of Balden and Roth [11], which are seen to be in good general agreement with our total C-production yields. Balden and Roth have estimated that wall sticking would reduce the total C-production observed by the QMS technique by up to 25% [11]. It is noted that a correction for such sticking and a correction for wall contributions, neither of which were made in the present measurements, would cancel each other out if they were of comparable magnitude, since they go in opposite directions. Regarding the yield variations evident for the different investigated C material, it is difficult to determine whether they are real, since they are generally smaller than the 40% estimated uncertainty for the total C-production yields. The apparent reasonable agreement between our own QMS results and the total weight loss measurements is in contrast to the QMS measurements of Balden and Roth [11], which were, however, not absolutely calibrated for CD_4, and did not make a separate measurement of the heavier hydrocarbon yields, but rather scaled their methane yields up by a factor of two to obtain an estimate of total C-production.

4.2. Transient measurements

To interpret the decay transients observed for the pre-loaded surfaces a simple model is used. We consider a slab of fixed scattering centers of initial excess density ρ_0 and thickness δ , exposed to an incident beam of current I and cross-sectional area A, i.e. having flux $\varphi = I/A$. By excess density is meant the density difference between the steady state densities reached by the 20 eV/D preparing beams and the higher-energy (either 80 eV/D or 150 eV/D) probing beams. The scattering centers refer to either trapped D atoms, or loosely bound hydrocarbons. The transient release rate of the ejected species of interest is given by $R(t) = A\delta\frac{d\rho}{dt}$. The density of the species of interest is given by $\frac{d\rho}{dt} = -\rho\sigma\phi$, where σ is taken to be the release cross-section, and has the solution $\rho = \rho_0 \exp(-\frac{t}{t_d})$, where the decay constant is given by $t_d = \frac{1}{\phi\sigma}$. The total release rate $R_T(t)$ is therefore $R_T(t) = R(t) + R_{ss}(E) = I\sigma\delta\rho_0 \exp(-\frac{t}{t_d}) + R_{ss}(E)$, where $R_{ss}(E)$ is the steady-state release rate of the high-energy species of interest. From fitting an $a + b\exp(-ct)$ analytical form to the observed time-dependent mass intensities (see Fig. 3), the ion-induced release cross-sections for the species of interest are obtained.

This model is obviously greatly over-simplified. The implantation slab thickness δ is not sufficiently small compared to the probing beam range to justify the implicit assumption that the probing beam passes through the prepared slab with constant energy. Indeed, at the low energies investigated, the straggling is comparable to the range (see, e.g. Fig. 3 of Ref [24]). It is therefore remarkable that, without exception, the transients are simple exponentials. Since the release cross-sections are highly unlikely to stay constant as the projectiles slow down, the simple exponential decay may be evidence for a strongly localized enrichment of D and hydrocarbons directly at the interface in response to low-energy beam preparation to steady-state conditions. Such super-saturation to D/C ratios of the order of unity at the surface vacuum interface has indeed been found in recent MD simulations [9,25].

The present measurements support the idea that during low-energy D-beam preparation, in addition to D inventory build-up, hydrocarbon precursors are formed that, at room-temperature, remain loosely bound in the prepared layer, and that their release is ion-induced. Such ion-induced release is not evident when starting the beam exposure from a virgin (as opposed to a beam-prepared) graphite surface, since the hydrocarbon emission as function of accumulated beam fluence starts in that case essentially from zero. It is noted that an ion-induced 'kinetic ejection' cross-section was explicitly incorporated into the chemical sputtering model of Mech et al. [3]. The present values are, however, about an order of magnitude larger than those deduced in [3]. Even though the projectiles of the present study are much lower in energy, the deduced D_2 release cross-sections are of similar magnitude as those previously reported [13,14].

The cross-sections tabulated in Table 1 were obtained for all three deuterium atomic and molecular species. Further, the cross-sections are given per D, i.e. normalized to the incident number of D atoms. It is seen from the table that the cross-sections/D generally increase with increasing number of D atoms in the incident projectiles, particularly at the 80 eV/D impact energy. This suggests that the D atoms comprising the incident projectiles may be not yet completely uncorrelated (i.e. dissociated) when inducing the hydrocarbon release, and may in part contribute the molecular-size effect recently observed in the methane production yield at low energies [26,27]. Also, in the case of the D^+ probing

Table 1
Atomic and molecular deuterium ion-induced cross-sections per D leading to emission of D_2 and selected hydrocarbons for normal impact on room-temperature ATJ graphite surfaces prepared by 20 eV/D D^+ beams (see text). Estimated cross-section uncertainties are shown in parentheses. Note: where entries are missing below, signal fluctuations prevented determination of the D_2 emission cross-sections.

Ions	Energy (eV/D)	Incident D flux (10^{-4} A/cm^2)	Preparing species (20 eV/D)	Cross-section/D (10^{-17} cm^2)			
				D_2	CD_4	C_2D_2	C_2D_4
D^+	80	4.87	D		2.6 (0.8)	2.3 (0.7)	1.9 (0.6)
D_2^+	80	3.10	D_2		4.4 (1.0)	3.1 (1.0)	2.6 (0.7)
D_3^+	80	2.73	D_3	12 (3.5)	6.8 (2.0)	4.1 (1.2)	4.8 (1.4)
D^+	150	4.21	D	6.3 (1.9)	3.6 (1.1)	2.9 (0.9)	3.9 (1.2)
D_2^+	150	2.74	D_2	15 (5)	13 (4.0)	5.4 (1.6)	7.9 (2.4)
D_3^+	150	3.69	D_3	7.4 (2.2)	8.4 (2.5)	4.0 (1.2)	5.8 (1.7)
D^+	80	2.92	D_2		4.7 (1.4)	3.8 (1.2)	7.2 (2.2)
D^+	150	1.34	D_2	21 (6)	8.8 (2.7)	5.0 (1.5)	7.6 (2.3)

beams, the surfaces were prepared both by 20 eV/D D^+ and D_2^+ beam irradiation. While equal steady-state hydrocarbon yields were found within the experimental uncertainty for the two differently prepared surfaces, the release cross-sections were found to be significantly higher (on the order of a factor of two) in the case of the molecular-ion-prepared surfaces. This difference is not understood at present, and may in part be a consequence of the over-simplified model used in the analysis.

5. Summary and conclusions

We have presented low energy steady-state chemical sputtering yields for the production of the CD_3 radical, CD_4, and heavier hydrocarbons. For energies below 100 eV/D the CD_3/CD_4 production ratio is found to be in the range 25–50% for all three C materials studied, indicating that stable CD_4 dominates CD_3 production for room-temperature graphite targets. From the summed hydrocarbon yields total C-production yields were determined which are found to be consistent with total mass loss measurements, but to be higher than earlier QMS-based measurements of both CD_4 and total C-production. In addition, cross-sections for ion-induced release of D_2, CD_4, C_2D_2, and C_2D_4 were determined from initial signal transients for 80 eV/D and 150 eV/D atomic and molecular D ions incident on graphite surfaces prepared by high-fluence exposure to 20 eV/D beams of the corresponding species. The transient measurements indicate that in addition to deuteration of the near surface region by the low-energy beams, loosely bound hydrocarbon precursors are produced, whose release is induced by the impacting projectiles. This release may in fact be localized at the surface/vacuum interface where strongly supersaturated deuteration conditions may exist.

Acknowledgements

HZ was appointed through the ORNL Postdoctoral Research Associates Program administered jointly by Oak Ridge Institute of Science and Education and Oak Ridge National Laboratory. This research was sponsored by the Office of Fusion Energy Sciences and the Office of Basic Energy Sciences of the US Department of Energy under contract No. DE-AC05-00OR22725 with UT-Battelle, LLC.

References

[1] G. Federici, Phys. Scr. T124 (2006) 1.
[2] W. Jacob, J. Roth, in: R. Behrisch, W. Eckstein (Eds.), Sputtering by Particle Bombardment: Experiments and Computer Simulations from Threshold to MeV, Springer, Berlin, 2007, p. 329.
[3] B.V. Mech, A.A. Haasz, J.W. Davis, J. Appl. Phys. 84 (1998) 1655.
[4] C. Hopf, A. von Keudell, W. Jacob, J. Appl. Phys. 94 (2003) 2373.
[5] J. Roth, J. Nucl. Mater. 266–269 (1999) 51.
[6] C. Hopf, W. Jacob, J. Nucl. Mater. 342 (2005) 141.
[7] J.H. Liang, M. Mayer, J. Roth, M. Balden, W. Eckstein, J. Nucl. Mater. 363–365 (2007) 184.
[8] E. Vietzke, J. Nucl. Mater. 290–293 (2001) 158.
[9] P.S. Krstic, C.O. Reinhold, S.J. Stuart, New J. Phys. 9 (2007) 209.
[10] F.W. Meyer, P.S. Krstic, L.I. Vergara, H.F. Krause, C.O. Reinhold, S.J. Stuart, Phys. Scr. T128 (2007) 50.
[11] M. Balden, J. Roth, J. Nucl. Mater. 280 (2000) 39.
[12] J. Roth, B.M.U. Scherzer, R.S. Blewer, D.K. Brice, S.T. Picraux, W.R. Wampler, J. Nucl. Mater. 93&94 (1980) 601.
[13] W.R. Wampler, S.M. Myers, J. Nucl. Mater. 111&112 (1982) 616.
[14] W.R. Wampler, B.L. Doyle, J. Nucl. Mater. 162–164 (1989) 1025.
[15] F.W. Meyer, H. Zhang, L.I. Vergara, H.F. Krause, Nucl. Instrum. and Meth. B 258 (2007) 264.
[16] F.W. Meyer, L.I. Vergara, H.F. Krause, J. Nucl. Mater. 337 (2005) 922.
[17] V.A. Morozov, F.W. Meyer, Rev. Sci. Instrum. 70 (1999) 4515.
[18] F.W. Meyer, L.I. Vergara, H.F. Krause, Phys. Scr. T124 (2006) 44.
[19] L.I. Vergara, F.W. Meyer, H.F. Krause, J. Nucl. Mater. 347 (2005) 118.
[20] B.V. Mech, A.A. Haasz, J.W. Davis, J. Nucl. Mater. 255 (1998) 153; B.V. Mech, PhD thesis, University of Toronto, 1997.
[21] C. Hopf, T. Schwarz-Selinger, W. Jacob, A. von Keudell, J. Appl. Phys. 87 (2000) 2719.
[22] M. Balden, J. Roth, E. De Juan Pardo, A. Wiltner, J. Nucl. Mater. 313–316 (2003) 348.
[23] G.M. Wright, A.A. Haasz, J.W. Davis, R.G. Macaulay-Newcombe, J. Nucl. Mater. 337–339 (2005) 74.
[24] W.R. Wampler, D.K. Brice, C.W. Magee, J. Nucl. Mater. 102 (1981) 304.
[25] E. Salonen, K. Nordlund, J. Keinonen, C.H. Wu, Phys. Rev. B 63 (2001) 195415.
[26] L.I. Vergara, F.W. Meyer, H.F. Krause, P. Träskelin, K. Nordlund, E. Salonen, J. Nucl. Mater. 357 (2006) 9.
[27] P.S. Krstic, C.O. Reinhold, S.J. Stuart, Eur. Phys. Lett. 77 (2007) 33002.